

Studies on the Pre-edge Region of the X-Ray Absorption Spectra of Copper(I) Oxide and the Diamminecopper(I) Ion

Arild Moen,* David G. Nicholson and Magnus Rønning

Department of Chemistry (AVH), University of Trondheim, N-7055 Trondheim, Norway

The distinctive pre-edge feature in the X-ray absorption spectra of copper(I) oxide and the diamminecopper(I) ion at the copper K-edge has been studied using synchrotron radiation. The relative intensities of these features, which are characteristic of copper(I) compounds, have been measured *via* the peak areas. The intensity of the oxide peak, with regard to the diammine and other two-coordinate copper environments, is anomalous, being reduced by *ca.* 60%. This is attributed to the macromolecular nature of the oxide, and the formation of intense excitons. Effects due to the small degree of non-stoichiometry may play an additional part in modifying pre-edge intensity by influencing the exciton lifetime.

The X-ray absorption spectra of copper(I) compounds at the K-edge contain an electronically interesting pre-edge feature at *ca.* 8984 eV. This feature is useful because it can yield structural and electronic information, especially when combined with the extended X-ray absorption fine structure (EXAFS) region of the same spectrum.¹ The peak is related to an absorption process that is often described in terms of single-particle transitions from a core state of essentially atomic-orbital character to appropriate unoccupied molecular orbitals of the unperturbed molecule. For solid macromolecular materials, the final states consist of unoccupied bands. This model also incorporates the relevant selection rules that govern a given transition. These rules are incorporated *via* the appropriate matrix elements that characterise the transition to the density of states (DOS). Hence, for K-edges, the 1s → 3d transitions that are often observed for transition-metal compounds can be related to vacancies in the 3d shell. Hence, a copper(I) 3d¹⁰ configuration has a zero probability for the latter transition occurring, whereas copper(II), with the 3d⁹ configuration, has a low probability for this transition.

In an extensive study of 19 copper(I) compounds, Kau *et al.*² showed that the intensity of the pre-K-edge peak decreases with increasing coordination to copper. With one notable exception, linear two-coordinate copper(I) compounds exhibit higher intensities than three- and four-coordinate systems. The exception is copper(I) oxide (Cu₂O) for which the pre-K-edge peak is considerably reduced in intensity relative to other linear two-coordinate systems. In pointing out the anomalous behaviour of copper(I) oxide, Kau *et al.* suggested that this material be studied further. Grioni *et al.*³ have shown that copper(I) oxide also behaves differently at the L_{2,3} (2p)-edge, the threshold intensity being enhanced relative to other copper(I) systems. In a more recent paper, Grioni *et al.*⁴ report that X-ray absorption spectroscopy (XAS) measurements at the copper L_{2,3}- and oxygen K-edges reveal unoccupied states of predominantly copper d and oxygen p character at the bottom of the conduction band. It was concluded, possibly because of what was termed the 'peculiar' Cu–O coordination, that the Cu 2p core-hole potential is stronger in copper(I) oxide than in other copper(I) materials. In this paper, we approach the anomalous L_{2,3}- (enhanced) and pre-K-edge (reduced) intensities of copper(I) oxide by considering the implications of both the macromolecular character of the material and the Cu–O interactions. XAS of the linear diamminecopper(I) cation helps to rationalise the observed results.¹

We report here an XAS study at the K-edge on macromolecular copper(I) oxide and, for purposes of comparison and calibration, the linear molecular system, copper(I) di-

amine cation [Cu(NH₃)₂]⁺. We also describe a procedure for extracting curve parameters that goes further than the method used by Kau *et al.* and which enables us to quantify more accurately the probability of spectral transitions, through the measurement of peak areas.

Experimental

Preparation

An aqueous solution containing the copper(I) diammine complex cation [Cu(NH₃)₂]⁺ (0.14 mol l⁻¹) was prepared as follows:

Cu(NO₃)₂ · 3H₂O (0.60 g) (Merck) was dissolved in water (5 ml) and 0.88 NH₃ (3 ml) added to give the deep-violet–blue tetraamminecopper(II) complex, [Cu(NH₃)₄]²⁺. (The initial precipitate of Cu(OH)₂ redissolved after all the ammonia solution had been added.) The pH of the solution was now adjusted (to pH 9) by adding HNO₃ (5 mol l⁻¹; 4.6 ml); the solution retained the blue colour characteristic of [Cu(NH₃)₄]²⁺. An aqueous solution of hydrazine was prepared by further diluting 35% aqueous hydrazine (Aldrich) by adding water (225 ml) to the commercial solution (25 ml). The tetraamminecopper(II) solution was reduced to diamminecopper(I) by adding 5.75 ml of the resulting hydrazine solution dropwise whilst the copper solution was shaken continuously. The solution effervesced (through the evolution of nitrogen) and at the end-point was almost colourless, with a slight yellow tinge and pH 9. This solution is shown below to contain the [Cu(NH₃)₂]⁺ complex ion. Hydrazine is a weaker Lewis base than ammonia and, therefore, does not compete with the latter in complexing copper(I).⁵ However, if the excess of hydrazine is higher than that given here, then the solution gradually darkens from yellow to brown and copper(I) oxide precipitates. Although the requisite excess of hydrazine reduces any dioxygen gas that reaches the solution, a longer-lasting solution is obtained if the additional precaution of purging air from the flask, with N₂, is performed. In this way, solutions have been prepared that last for over a week, although the solutions used in this work were prepared only a few minutes before being placed in the synchrotron beam.

Copper(I) oxide was obtained from Aldrich Chemical Co., Ltd. Iron(III) phosphate with the berlinite structure⁶ was used to check the resolution of the spectrometer; it was prepared by the method of Royen and Korinth.⁷ Zinc acetate was used to check the modelling of the pre-edge background, and was prepared according to Clegg *et al.*⁸

X-Ray Absorption Spectra

XAS results were collected at the European Synchrotron Radiation Facility on the Swiss–Norwegian beamline. During

data collection, the synchrotron was operated at 6 GeV, with a ring current of 85–130 mA. The monochromator was a channel-cut Si(111) single crystal. Higher-order harmonics (*ca.* two orders of magnitude) were rejected by means of a chromium-coated mirror. The maximum resolution ($\Delta E/E$) of the Si(111) bandpass was 1.4×10^{-4} . Since the vertical fan of radiation was small the resolution was essentially determined by the bandpass. The beam size was defined by the slits in the station. The vertical aperture was 0.5 mm and the vertical divergence is defined by a 0.5 mm aperture, 35 m from the source point. Data were collected at the iron and copper K-edges (7112 and 8982 eV, respectively) in the transmission mode, using an unfocussed incident beam of dimensions 0.6×4.7 mm. N_2 -filled ion chambers were used for measuring the intensities of the incident and transmitted X-rays. Data were collected in steps of 1/8 eV, the energy being calibrated using the model compounds, and the absolute energy scale chosen to be the value of the absorption maximum at 8991.8 eV for copper(I) oxide. Reproducibility in the edge position was estimated to be *ca.* 0.15 eV. The amount of material used to prepare the samples for transmission XAS was calculated from the element-mass fractions of the compounds and the absorption coefficients of the elements⁹ just above the absorption edge, to give $\ln(I_0/I)$ of almost unity. The well powdered (diameter of *ca.* 50–100 μm) samples were mixed with boron nitride, so as to obtain a homogeneous (no pinholes) sample thickness of *ca.* 1 mm for a surface area of 1.2 cm^2 , and placed in aluminium sample holders and held in place by Kapton tape. Details concerning the copper(I) diammine solution and data collection are given in ref. 1.

The monochromator delivers radiation with a Gaussian distribution,^{10–12} and full width at half-height (FWHM) of *ca.* 1.0 and 1.3 eV at the iron and copper K-edges, respectively (see above for the resolution). This monochromator has also been used for high-resolution X-ray diffraction studies. Even at the best angular resolution, in diffraction peaks at high values of 2θ , no evidence of any beam distortion, or instability due to the heat load from the white beam has been observed. The monochromator was directly cooled by passing chilled water through a 20 mm diameter bore. The experimental energy band is convoluted with the width of the 1s core level. The transition probabilities of the latter depend on the core-hole lifetime and are described by a Lorentzian function¹⁰ with FWHM of *ca.* 1.1–1.2 and 1.5 eV for iron and copper, respectively.^{13,14} Note that for emissions involving longer-lived states *e.g.* the valence state, there is a significant Gaussian contribution in the final state.

Data Reduction

Data were summed, corrected for dark currents, and converted to energy, and a linear background was then fitted to the featureless pre-edge region and subtracted. The resulting spectra were consistently normalised to the midpoint of the first EXAFS oscillation. The pre-edge region, extending to unit absorption at the edge, was used in the pre-edge fits.

Curve Fitting (Background and Pre-edge Peak)

The background was fitted to a pseudo-Voigt function (a composite Lorentzian and Gaussian function, see below). Fig. 1 shows such a background-fit to the pre-edge region of zinc acetate. This edge was chosen because zinc(II) is isoelectronic with copper(I), but does not show the pre-edge peak, thereby allowing the background to be characterised unimpeded by extra spectral features. Fig. 1 demonstrates that a good fit of the theoretical background to an experimental background has been achieved by using the pseudo-Voigt function. This function was therefore used to model the background of the copper edges, through similar individual least-squares fit-

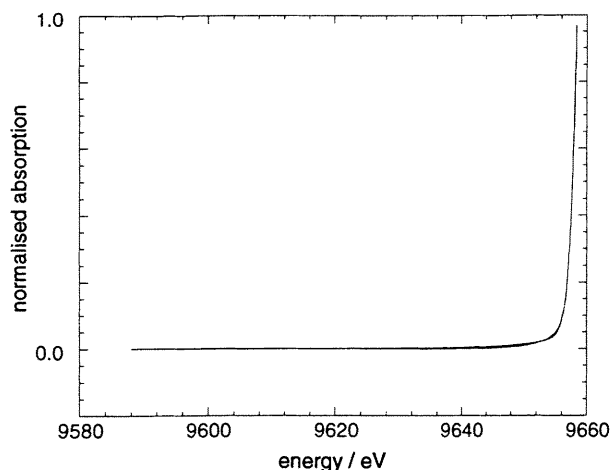


Fig. 1 Zinc K-edge region of the X-ray absorption spectrum of zinc acetate, showing the result of the background fit to the pseudo-Voigt function. On this scale, the theoretical curve almost completely overlaps the experimental curve. The former, which is barely discernible from the latter, is the lower of the two. $\chi^2 = 0.0015$.

tings, for the copper edge spectra. The Cu^{I} pre-edge peaks were also least-squares fitted to a pseudo-Voigt function. The intensities, in the form of areas, were calculated by trapezoidal integration.

Checking the Fitting Procedure

For comparison and calibration purposes, the 1s–3d pre-edge peak of iron(III) phosphate (FePO_4), berlinite, was measured using the same procedures. We found a pre-edge peak with FWHM of 1.7 eV. (Deconvoluting the contribution from the optics yields a spectral FWHM of 1.4 eV.) It is known that this peak arises from allowed transitions from the 1s orbital to the valence e and t_2 symmetry orbitals associated with the T_d point symmetry, the energy difference between the two transitions being unresolved. This result compares favourably with that of Calas and Petiau¹⁵ (FWHM = 1.9 eV) for a similar environment, but measured at a somewhat lower resolution. [We note that the transitions can be resolved (0.55 eV splitting) by optical absorption spectroscopy.¹⁶]

Discussion

Depending on the element, the pre-edge region of an X-ray absorption spectrum sometimes contains features of structural or electronic interest. Thus, features close to the absorption edge often can be related to electronic transitions from 1s or 2p orbitals (K- or L-edges, respectively) to higher bound states, the energies of which lie within the discrete part of the spectrum. The edge itself defines the threshold ionisation energy, above which lies the continuum with oscillations (XANES and EXAFS) superimposed on a smoothly varying background of photoelectron energy. These oscillations, or fine structure, reflect the electronic and geometric characteristics of the molecular environment of the selected atom. In this paper, we are concerned with the discrete part of the spectra of linear copper(I) environments, and their characteristic pre-edge features.

The X-ray absorption spectra of copper(I) species are particularly rich in information compared to those of copper(II), because they exhibit a pre-edge peak at *ca.* 8984 eV that is characteristic of monovalent copper [Fig. 2(a)] and which is sensitive to the metal's environment. In general, the main electronic transitions following the absorption of an X-ray photon are dipolar or quadrupolar, and the selection rules governing such transitions depend on the symmetry group of the coordinated species. For quadrupolar transitions, the

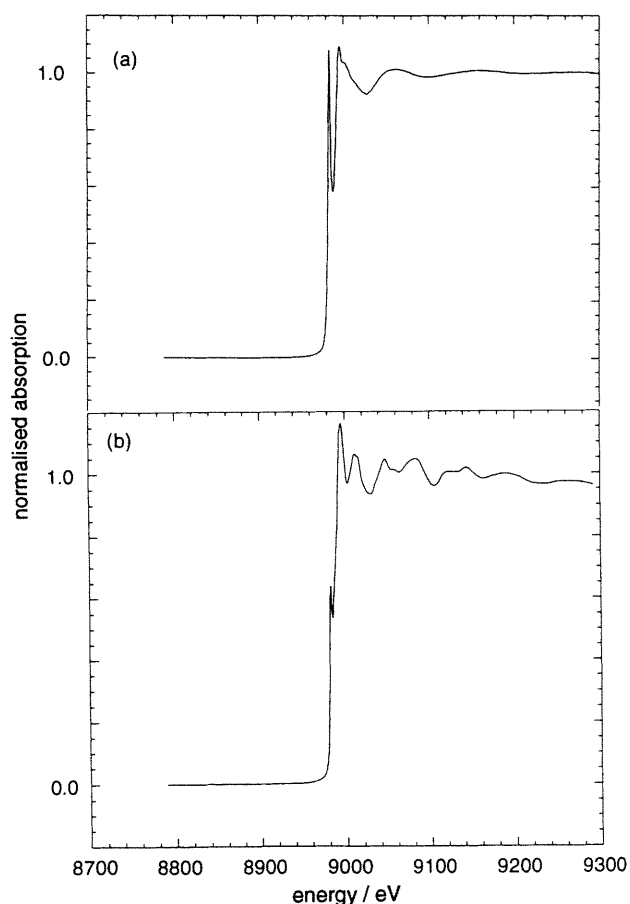


Fig. 2 Part of the X-ray absorption spectrum of (a) the diamminocopper(I) ion and (b) copper(I) oxide, showing the pre-edge features

selection rules are $g \rightarrow g$; $u \rightarrow u$ ($\Delta L = 0$), and for dipolar transitions $g \rightarrow u$ ($\Delta L = \pm 1$).¹⁷ The high intensity of the copper(I) pre-edge peak is consistent with the electric dipolar transitions $1s$ (K-edge) $\rightarrow 4p$ and $1s \rightarrow$ ligand group orbitals, since electric quadrupolar transitions are considerably weaker. Polarised single-crystal studies (ref. 2 and references cited therein) on two copper(I) complexes show that the pre-edge peak is (x, y) -polarised. This allows the pre-edge peak to be assigned to the $1s \rightarrow 4p_{x,y}$ electric-dipole allowed transition.

A particularly useful characteristic of the pre-edge peak is its sensitivity to coordination about copper(I); the intensity of the transition at *ca.* 8984 eV, decreases with increasing coordination number around the metal.² This is attributed to the increased coordination (with an attendant overall covalency) which reduces the metal character of the $4p$ orbitals, as their contribution to the molecular orbitals and ligand bonding is enhanced. This results in the probability of the transition varying with the geometry and covalency. In the case of K-edges, the intensity of the transition is proportional to the square of the modulus of the transition dipole moment, $|\mu|^2$, the transition dipole moment, μ , taking the form:

$$\mu_{1s \rightarrow 4p} = -e \int \psi_{4p}^* r \psi_{1s} d\tau$$

where ψ_{1s} and ψ_{4p} are the initial and final wavefunctions of the copper(I) system, respectively. For allowed dipole transitions, the final wavefunction must be p-like, in accordance with the selection rules for the l quantum number. Clearly, the intensities, *i.e.* areas, of the pre-edge peaks for normalised spectra are measures of the transition probabilities. Kau *et al.*² reported a difference-edge-analysis procedure that

involved normalising the copper edge of the unknown copper(I) sample, followed by subtracting the normalised edge of a copper(II) reference. This resulted in a derivative-shaped peak, where the peak height at 8984 eV was correlated with the coordination number and geometry. A more correct measure of transition probabilities is the peak area (this parameter is also less sensitive to differences in resolution), but since the background removal associated with this method introduces artefacts originating from mismatches between the backgrounds of both spectra, somewhat distorted peak heights have to be used.

In this paper, we describe a least-squares background treatment that is more accurate (because the above extraneous features are not introduced) followed by least-squares fitting the pre-edge peak to a pseudo-Voigt function. The advantage of this method is that several parameters are made available. These are: the intensity, position, FWHM and peak area. The normalised spectra and the least-squares fits of pseudo-Voigt functions to both the pre-edge region backgrounds and to the peaks of copper(I) diammine and copper(I) oxide spectra are shown in Fig. 3(a) and (b), respectively, with the values of the FWHM, intensity and peak area being given.

The FWHM is an important parameter which is governed by several contributions. Aside from the resolution of the instrumentation, the major contribution to the linewidth is the lifetime of the $1s$ core-hole, and of the promoted electron in the $4p$ levels. Additional sources of broadening include 'many-body' effects, *e.g.* the influence of the core-hole on the band states may be significant. In addition to these intrinsic contributions, there is an addition to the width that arises from experimental limitations, mainly the resolution of the spectrometer. The experimental contribution to the FWHM is introduced by convoluting the spectral Lorentzian distribution with a Gaussian or Gaussian-Lorentzian spread of energies. The resolution of the present arrangement is *ca.* 1.3 eV at 9 keV (see Experimental).

The results show that the FWHM for the diammine complex and the oxide are the same, within experimental error. The measured values (3.0–3.2 eV) reduce to *ca.* 2.7 eV when the profile due to the optics of the spectrometer is deconvoluted from the measured peaks. This value is large, perhaps concealing an unresolved splitting of the $4p$ orbitals [*i.e.* $4p_x, 4p_y$ (degenerate) and $4p_z$]. The similar FWHM for the molecular and macromolecular systems is consistent with the similar metal characters of the $4p$ levels in both compounds, and with their non-bonding nature. It is important to use peak areas (intensities) and not peak heights, because particular combinations of height and FWHM give the same area and the reduced peak height in the oxide spectrum cannot be assumed *a priori* to indicate a smaller peak area. In fact, it transpires that the peak area or intensity is considerably reduced relative to the diammine complex. This indicates a lower transition probability for the oxide. Since the immediate environments of the copper atoms in both systems are similar, the difference must be rationalised by considering the extended copper(I) oxide structure.

Copper(I) Oxide and the Diamminocopper(I) Cation

Copper(I) oxide is a yellow or red material (the colour difference being due to the particle size) with a narrow range of homogeneity represented by the formula $\text{Cu}_{2-\delta}\text{O}$. The material has long been regarded as a prototype of oxides whose properties are governed by their departure from exact stoichiometry, in the direction of metal deficiency.¹⁸ The non-stoichiometry, δ , of $\text{Cu}_{2-\delta}\text{O}$ has been studied by a variety of methods that include chemical analysis of a quenched sample, thermogravimetry, electrical resistivity measurements and

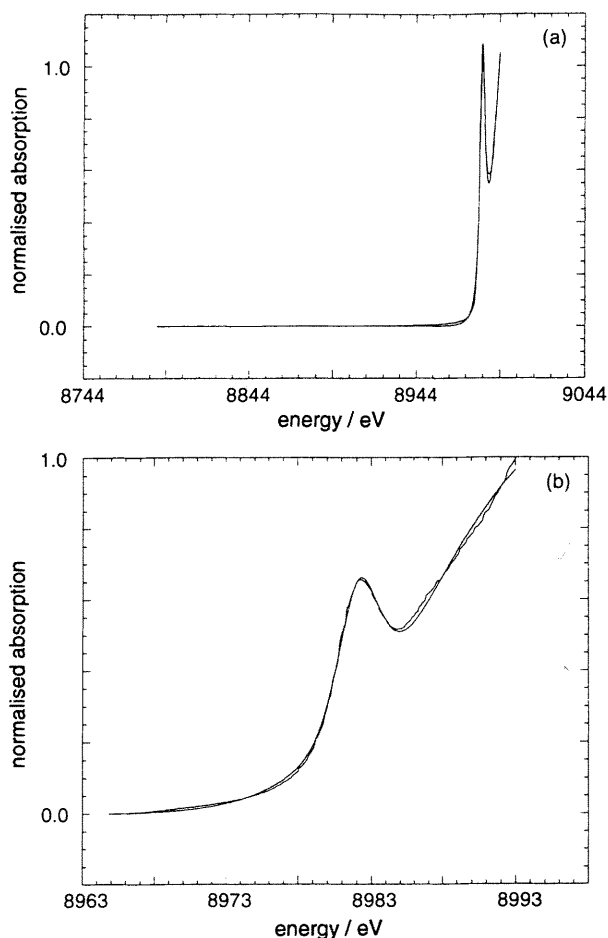


Fig. 3 Pre-edge regions of the XAS of (a) diamminocopper(I) ion and (b) copper(I) oxide showing the fits to pseudo-Voigt function. The close fit between the theoretical and experimental curves is evident; the former, which in places is only barely discernible from the latter, is the lower of the two. (b) is drawn on an expanded energy scale relative to (a) in order to illustrate the quality of the fit. (a) $\chi^2 = 0.0094$, FWHM = 3.20(8) eV, peak energy = 8983.64(2) eV, peak height = 0.89(7) eV and intensity (peak area) = 3.6(2). (b) $\chi^2 = 0.024$, FWHM = 2.96(3) eV, peak energy = 8982.93(1) eV, peak height = 0.384(8) and intensity (peak area) = 1.4(2).

coulometric titration. These results were not consistent.¹⁹ $\text{Cu}_{2-\delta}\text{O}$ is a metal-deficient p-type semiconductor with cation vacancies. The deficiency in copper leads to formal charge compensation by a corresponding number of metal atoms being oxidised to copper(II). This results in the copper(I) content being further decreased (by δ) to 2δ , with the above formula being rewritten as $[\text{Cu}^I]_{2-2\delta}[\text{Cu}^{II}]_{\delta}\text{O}$. Since δ is small, non-stoichiometry is apparently only a minor factor which by itself cannot explain the decrease in intensity of the pre-edge peak, but it may have a more significant role to play by influencing the lifetimes of excitons (see below), and through that mechanism, the pre-edge peak intensity.

In copper(I) oxide²⁰ (Fig. 4) each copper atom forms two collinear bonds to oxygen, and each oxygen atom is tetrahedrally linked to four copper atoms in a cubic crystal structure (O_h^4). The copper and oxygen atoms are linked together in exactly the same way as found for the oxygen and silicon atoms, respectively, in cristobalite. However, the Cu–O (1.85 Å) distance is appreciably longer than the Si–O distance (1.55 Å). As a result, a Cu_2O framework based solely on the cristobalite structure would have much unoccupied space. Instead, some of this volume is taken up by a second identical framework interposed within the volume occupied by the

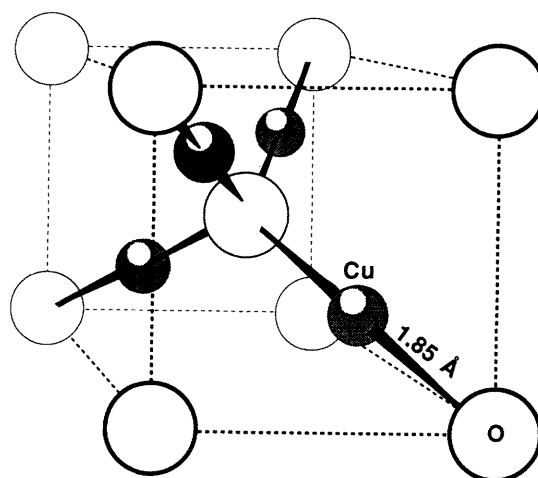


Fig. 4 One of the two identical interpenetrating substructures of the copper(I) oxide lattice

first. In other words, the crystal consists of two interpenetrating lattices which are not connected by any primary (Cu–O) bonds. The two individual structures must therefore be held together by the total sum of relatively weak secondary interactions, the largest being due to the Cu...Cu distance (3.017 Å), which is considerably longer than that found in the metal itself (2.56 Å). Copper(I) oxide is a semiconductor with a bandgap $E_g = 2.17$ eV.²¹ Since the copper atoms are monovalent they contain the filled formal $3d^{10}$ closed shell, and there are consequently no $1s \rightarrow 3d$ transitions. [This, of course, also applies to the copper(I) diammine cation.]

One of the earliest descriptions of the bonding in copper(I) oxide was presented by Orgel²² in the form of a qualitative, and essentially ionic, ligand field model for copper(I) oxide (which can also be used for the diammine) that takes into account the diamagnetic and semiconducting properties of the material. Instead of a spherically symmetric d^{10} state, the Cu^+ cation is described as $(d)^8(3d_{z^2} 4s)^2$. The $3d_{z^2} 4s$ hybridisation has the effect of transferring electron density from the bond axis, which is aligned along the z -direction, to the $4s$ orbital. The short Cu–O bond was explained by invoking this hybridisation, in which the diffuse nature of the $4s$ orbital enables the O^{2-} anions to approach the copper ion more closely than the distance given by the sum of the ionic radii. Restori and Schwarzenbach have studied the charge densities in copper(I) oxide using X-ray data.²³ Their results indicate a deficit of charge density along the linear O–Cu–O bond axis, which was interpreted as being due to $\alpha\psi(3d_{z^2}) + \beta\psi(4s)$ hybrid orbitals, with $|\beta/\alpha| = 0.7(2)$.

Another copper(I) species with the same linear coordination is the copper(I) diammine cation, in which the Cu^I–N bond lengths are 1.88 ± 0.02 Å.¹ This is similar to the Cu–O bond length of 1.85 Å in copper(I) oxide.²⁴ However, despite having similar bond lengths, there is a significant difference between their pre-edge X-ray absorption spectra, as mentioned above.

The structural similarity of the copper environments in the oxide macromolecule and the diammine molecular cation, together with the similar copper–ligand bond distances, suggest that a similar bonding description can be used for both the diammine complex and a $\text{Cu}(\text{OCu}_3)_2$ fragment in the oxide. Indeed, the diammine is the key to rationalising the bonding in the oxide, and Orgel's model and the description of Restori and Schwarzenbach can be translated into the schematic molecular-orbital level diagram shown in Fig. 5 for copper in both environments. The figure summarises the irreducible transformations of the atomic orbitals according to the $D_{\infty h}$ point group. Clearly there is appreciable covalent

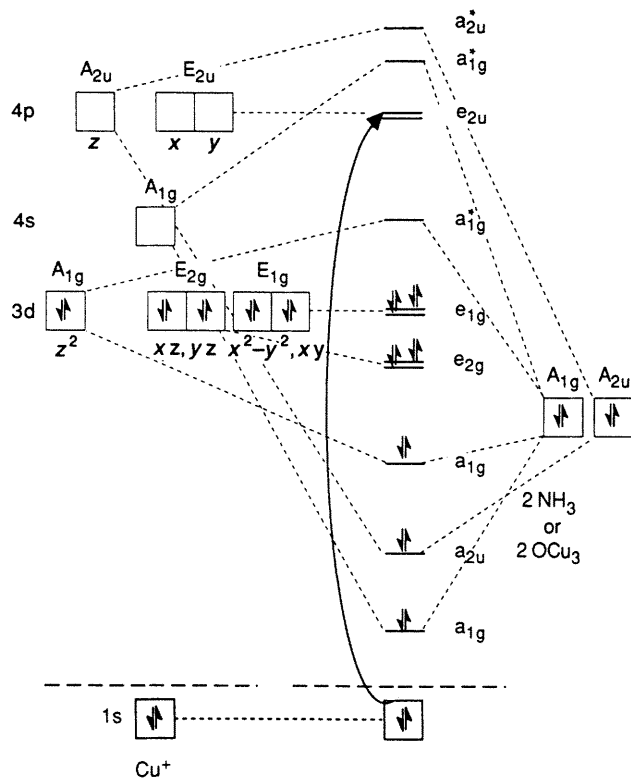


Fig. 5 Schematic orbital-energy-level diagram for $[\text{Cu}(\text{NH}_3)_2]^+$ or the $[\text{Cu}(\text{OCu}_3)_2]$ fragment, showing the transition of the Cu 1s electron to the nonbonding e_{2u} ($4p_x, p_y$) orbital

character in the bonding in the diammine, in view of the coordinate bonds between copper and the ammonia ligands. This makes the more extreme and simplistic ionic picture inappropriate. The similarity between the metal environments in the diammine complex and the oxide $[\text{Cu}(\text{OCu}_3)_2]$ fragment is consistent with a similar bonding situation for the latter, and this is supported by the similar energies of the Cu 3d and O 2p levels, which causes these levels to mix extensively.²⁵ The relevance of the molecular-orbital description of the molecule or fragment to the condensed, extended copper(I) oxide lattice (Fig. 6) has been demonstrated by Hoffman and Zheng²⁶ (in another example) to be a particu-

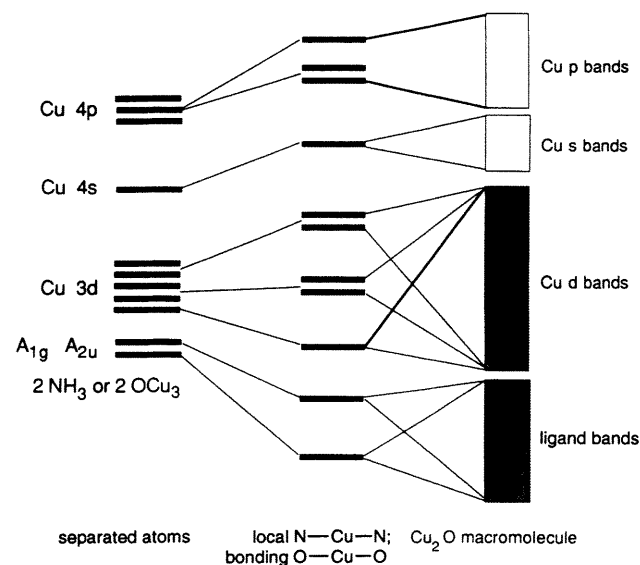


Fig. 6 Schematic picture of the band structure in the macromolecule Cu_2O and its relation to the MO diagram for the $[\text{Cu}(\text{OCu}_3)_2]$ fragment

larly graphic way of illustrating that, with respect to bonding considerations, what applies to the inorganic solid is similar to what applies to the isolated molecule.

The Pre-K-edge Intensities of Copper(I) Oxide and the Diamminecopper(I) Cation: Exciton Formation

It seems reasonable to infer from the structural data that the difference between the intensities (*i.e.* areas) of the pre-edge peaks in the diammine complex and oxide is rooted in their molecular and macromolecular characters, respectively, and not to any significant differences in the Cu–N and Cu–O bonding. It is the different behaviours of the electron–hole pair, that arises out of the $1s \rightarrow 4p$ excitation, for the two compounds that is reflected in the different intensities of the pre-edge peak. Whereas in the diammine complex there are essentially no interactions between individual $[\text{H}_3\text{N}-\text{Cu}-\text{NH}_3]^+$ molecular ions (they are in aqueous solution) and the electron–hole pair is localised on its original molecule, in the oxide, the situation is very different because here there are interactions between linked $[\text{Cu}_3\text{O}-\text{Cu}-\text{OCu}_3]$ groupings that permit each electron–hole pair to hop from grouping to grouping. The two independent lattices in the oxide are a factor in this migration, which constitutes an exciton of which there are two kinds; Frenkel excitons and Wannier excitons.^{27,28} The former are tightly bound electron–hole pairs while the latter are loosely bound pairs. The exciton carries the energy of the photon that created it, and is a quantum of electronic excitation whose motion is characterised by a wave vector.²⁹ The energy separation between the 1s and 4p levels, and the shielding between these levels, by the intervening filled orbitals, makes the hole–electron binding weak and the exciton is Wannier-like. A strong interaction between molecules or groupings leads to fast migration, whereas a weak interaction (as is the case for the diammine with an intense pre-edge peak) implies that the exciton is localised on its original molecule, in which case it is an ordinary excitation. The formation of excitons causes lines to shift in energy, and intensities to change. The intensity of the pre-edge in the solution spectrum of the diammine is at a maximum because the transition is an ordinary excitation, whereas the strong interactions in the solid-state oxide are associated with rapid migrations of electron–hole pairs, and the production of intense excitons.

Copper(I) oxide is particularly interesting in the context of exciton formulation because it is known that the higher excitation densities in that material produce excitons with long lifetimes.^{30,31} Attention has been focussed on copper(I) oxide as a crystal in which Bose–Einstein condensation of excitons might be observable.^{32,33} The intensity of optical absorption by excitons has been studied by Elliot, and subsequently by Baumeister.^{34,35} It is the long exciton lifetime in copper(I) oxide, together with the intensity of the exciton formation, that is the reason behind the observed reduced pre-edge intensity. Imperfections in the crystal structure (*e.g.* non-stoichiometry) affect the lifetime, and synthetic crystals have shorter lifetimes than naturally grown crystals.³¹ Non-stoichiometry is also relevant, and it would be interesting in this context to compare the intensities of the pre-edge peak for natural and synthetic samples of copper(I) oxide. The two independent, interposed lattices that constitute the overall Cu_2O lattice clearly play a role in the migration and interaction of the excitons. For photon fluxes above a critical level (defined by the exciton lifetime), exciton production is high enough to reduce the overall probability of the $1s \rightarrow 4p$ transition. The weak linking between the electron and its hole, which characterises a Wannier exciton means that both are

not necessarily localised at the same instant on the same atom. The migration velocities of electron and hole, and their lifetimes, reduce the transition probabilities in both cases, and the cumulative effect of this dynamic process is manifested by the lower intensity of the pre-edge peak, relative to the diammine. This is quantified by the ratio of the intensities (*i.e.*, peak areas) of the two systems (0.4).

Conclusion

We have measured the intensity (peak area) and width (FWHM) of the pre-K-edge peak at *ca.* 8984 eV in the X-ray absorption spectrum of copper(I) oxide relative to that for the diammine copper(I) complex, the peak height of the latter being normalised. The peak areas are 1.4 and 3.6, respectively, with similar widths (3.0 and 3.2 eV, respectively). Correcting the widths for optical broadening yields a large spectral width of *ca.* 2.7 eV for both spectra.

Previous studies on copper(I) complexes show that the copper pre-K-edge peak at *ca.* 8984 eV is sensitive to coordination number and the geometry about the copper(I) ion. This is attributed to the decrease in metal character of the 4p orbitals, as overall participation in metal–ligand bonding increases.

However, the present analysis of copper(I) oxide shows that for this macromolecular material at least, the pre-K-edge peak in copper(I) compounds cannot always be used to give stereochemical information. In cases where there are strong interactions between molecular groupings, indirect energy transfer *via* exciton mechanisms can be a complicating factor. Therefore, using the pre-edge peak area information as a stereochemical indicator is valid only for those systems in which these interactions in the solid-state materials are known to be absent or insignificant.

In the case of copper(I) oxide, non-stoichiometry (albeit small) could, in principle, be an additional contributing factor in reducing the peak intensity. Indeed, the presence of copper(II) atoms that occupy the copper(I) vacancies also modifies the band structure, and can be envisaged as playing a more extensive role in exciton mechanisms. The provenance of copper(I) oxide samples in XAS studies is thus relevant, and detailed experiments on samples in which the stoichiometry is carefully established and controlled might give supplementary information of interest.

We are intrigued by the fact that the crystal structure of copper(I) oxide consists of two independent (in the sense that there are no primary linkages between them), but interpenetrating Cu₂O substructures. Although Restori and Schwarzenbach²³ suggest that the Cu··Cu interactions are not important for the stability of the structure, the consequences of this structural property on other properties of the oxide do not appear to have received particular attention. Any theoretical treatment of interactions in this material should involve this feature. Indeed, we suggest that copper(I) oxide is an interesting candidate for more detailed experimental, and also theoretical, studies on its electronic behaviour, including the generation and propagation of excitons. More detailed studies on the relationship between exciton formation and pre-edge peak intensity could be carried out on naturally grown single crystals and also on synthetic samples, (in which the metal deficiency is established).

We thank the Research Committee, University of Trondheim and the Norwegian Research Council for grants towards constructing the Swiss–Norwegian Beamline. This is contribu-

tion No. 95-2 of the Swiss–Norwegian Beamline at the ESRF. We also appreciate grants from Statoil (VISTA), the Nansen Foundation and the Lise and Arnfinn Hejes Foundation. We also thank the Project Team (E. Blanc, H. Emerich, J. Mårdalen, P. Pattison and H. P. Weber) of the Swiss–Norwegian Beamline, ESRF, for their dedicated support. Constructive discussions with Dr. Wendy Flavell, Professors Razi Naqvi, Frode Mo and Reidar Stølevik are gratefully acknowledged.

References

- 1 G. Lamble, A. Moen and D. G. Nicholson, *J. Chem. Soc., Faraday Trans.*, 1994, **90**, 2211.
- 2 L-S. Kau, D. J. Spira-Solomon, J. E. Penner-Hahn, K. O. Hodgson and E. I. Solomon, *J. Am. Chem. Soc.*, 1987, **109**, 6433.
- 3 M. Grioni, R. Schoorli, J. B. Goedkoop, J. C. Fuggle, F. Schafer, E. E. Koch, G. Rossi, J-M. Esteve and R. Karnatak, *Phys. Rev. B*, 1989, **39**, 1541.
- 4 M. Grioni, J. F. van Acker, M. T. Czyzyk and J. C. Fuggle, *Phys. Rev. B*, 1992, **45**, 3309.
- 5 N. N. Greenwood and A. Earnshaw, *Chemistry of the Elements*, Pergamon Press, Oxford, 1993.
- 6 Hok Nam Ng and C. Calvo, *Can. J. Chem.*, 1975, **53**, 2064.
- 7 P. Royen and T. Korinth, *Z. Anorg. Allg. Chem. A*, 1969, **30**, 340.
- 8 W. Clegg, I. R. Little and B. P. Straughan, *Acta Crystallogr., Sect. C*, 1986, **42**, 1701.
- 9 *International Tables for X-Ray Crystallography*, ed. J. S. Kasper and K. Lonsdale, The Kynoch Press, Birmingham, 1959.
- 10 B. K. Agarwal, *X-Ray Spectroscopy*, Springer-Verlag, Berlin, 1979, p. 276.
- 11 T. A. Tyson, A. L. Roe, P. Frank, K. O. Hodgson and B. Hedman, *Phys. Rev. B*, 1989, **39**, 6305.
- 12 F. W. Lytle, *Applications of Synchrotron Radiation*, ed. H. Winick, D. Xian and M. H. Huang, Gordon and Breach, New York, 1989, p. 135.
- 13 L. G. Parratt, *Rev. Mod. Phys.*, 1959, **31**, 616.
- 14 J. E. Muller, O. Jepsen and J. W. Wilkins, *Solid State Commun.*, 1982, **42**, 365.
- 15 G. Calas and J. Petiau, *Solid State Commun.*, 1983, **48**, 625.
- 16 A. S. Marfunin, *Physics of Minerals and Inorganic Materials. An Introduction*, Springer-Verlag, Berlin, 1979.
- 17 P. Berthet, J. Berton and F. d'Yvoire, *Mater. Res. Bull.*, 1988, **23**, 1501.
- 18 M. O'Keefe and W. J. Moore, *J. Chem. Phys.*, 1961, **35**, 1324.
- 19 A. Kosuge, *Chemistry of Nonstoichiometric Compounds*, Oxford University Press, London, 1994.
- 20 A. F. Wells, *Structural Inorganic Chemistry*, Clarendon Press, Oxford, 1984.
- 21 B. K. Agarwal, C. B. Bhargava, A. V. Vishnoi and V. P. Seth, *J. Phys. Chem. Solids*, 1976, **37**, 725.
- 22 L. E. Orgel, *J. Chem. Soc.*, 1958, 4186.
- 23 R. Restori and D. Schwarzenbach, *Acta Crystallogr. Sect. B*, 1986, **42**, 201.
- 24 B. Morosin, *Acta Crystallogr., Sect. B*, 1969, **25**, 19.
- 25 J. E. Huheey, E. A. Keiter and R. L. Keiter, *Inorganic Chemistry. Principles of Structure and Reactivity*, Harper Collins College Publishers, New York, 1993.
- 26 R. Hoffman and C. Zheng, *J. Phys. Chem.*, 1985, **89**, 4175.
- 27 J. Frenkel, *Phys. Rev.*, 1931, **37**, 1276.
- 28 G. H. Wannier, *Phys. Rev.*, 1937, **52**, 191.
- 29 D. L. Dexter and R. S. Knox, *Excitons*, Interscience Publishers, New York, 1965.
- 30 D. W. Snoke, J. P. Wolfe and A. Mysyrowicz, *Phys. Rev. B*, 1990, **41**, 11171.
- 31 J. P. Wolfe, *J. Lumin.*, 1992, **53**, 327.
- 32 A. Mysyrowicz, D. W. Snoke and J. P. Wolfe, *Phys. Status Solidi B*, 1990, **159**, 387.
- 33 D. Hulin, A. Mysyrowicz and C. Benoit a la Guillaume, *Phys. Rev. Lett.*, 1980, **45**, 1970.
- 34 R. J. Elliot, *Phys. Rev.*, 1957, **108**, 1384.
- 35 P. W. Baumeister, *Phys. Rev.*, 1961, **121**, 359.